NESTIN-GFP TRANSGENE LABELS SKELETAL PROGENITORS IN THE PERIOSTEUM

Guillaume Tournaire[a,b], Steve Stegen[a,b], Greta Giacomini[a], Ingrid Stockmans[a], Karen Moermans[a], Geert Carmeliet[a,b] and Nick van Gastel[a,b]

[a] Laboratory of Clinical and Experimental Endocrinology, Department of Chronic Diseases, Metabolism and Ageing, KU Leuven, Leuven, Belgium

[b] Prometheus, Division of Skeletal Tissue Engineering, KU Leuven, Leuven, Belgium

Corresponding author:

Geert Carmeliet, MD, PhD

Laboratory for Clinical and Experimental Endocrinology

Department of Chronic diseases, Metabolism and Ageing

Herestraat 49, 3000 Leuven, Belgium

Tel: +32 16 331731

Email: geert.carmeliet@kuleuven.be

32

Abstract

The periosteum is critical for bone repair and contains skeletal stem cells (SSCs), but these cells are still poorly characterized. In the bone marrow, cells expressing the Nes-GFP transgene have been described to be SSCs. Here, we investigated whether Nes-GFP expression also typifies SSCs in the periosteum. We show that in adult mice, Nes-GFP cells are present in the periosteum and localize closely to blood vessels, but periosteal Nes-GFP cells express SSC and progenitor markers differently compared to Nes-GFP cells in the bone marrow. Periosteal Nes-GFP cells show *in vitro* clonogenicity and tri-lineage differentiation potential and they can form bone *in vivo*. Shortly after fracture, they start to proliferate and they contribute to the osteoblast pool during the repair process. However, periosteal Nes-GFP cells are not slow dividing nor self-renewing *in vivo*. These results indicate that in adult mice, periosteal Nes-GFP expressing cells are skeletal progenitors rather than true SSCs, and they participate in the fracture healing process.

Highlights

- Periosteal Nes-GFP cells express SSC markers differently compared to their bone marrow counterpart
- Periosteal Nes-GFP cells show properties of skeletal progenitors *in vitro*
- Periosteal Nes-GFP cells can form bone *in vivo*, but lack the characteristics of true SSCs
- During fracture repair, Nes-GFP cells start to proliferate and become osteoblasts in the fracture callus

Keywords

Nestin; Periosteum; Skeletal stem cell; Skeletal progenitors; Osteoprogenitors; Bone repair

1. Introduction

The bone is a rigid but dynamic tissue with a continuous turnover and a high regenerative potential. Self-renewing skeletal stem cells (SSCs) are found in the bone marrow compartment and are characterized by clonogenicity and the ability to differentiate into several mesodermal cell lineages like chondrocytes, osteoblasts and adipocytes [1–3]. However, the contribution of bone marrow-derived cells to fracture repair is limited [4]. Instead, the periosteum, the membrane lining the outer bone surface, provides the majority of cells forming the fracture callus [4–6]. Additionally, transplanting periosteum-derived cells (PDCs) at an ectopic site induces new cartilage and bone formation with superior capacity compared to bone marrow-derived stromal cells [7,8]. These data suggest that next to the bone marrow, a second SSC compartment exists in the periosteum, which is of interest for regenerative medicine. However, characterization of periosteal stem cells is still limited.

During recent years, several markers and combinations thereof have been described that label SSCs, including Nestin, Leptin receptor (LepR) [9], CD105 [10,11], CD51 [10,12], CD200 [12], PDGFRα [13,14] and Sca1 [13,14]. Nestin is a cytoskeletal protein that belongs to the family of intermediate filaments and is expressed in a variety of stem and progenitor cells as well as in several types of cancer cells [15]. In the bone marrow, cells expressing green fluorescent protein (GFP) under the control of the regulatory elements of the Nestin promotor/enhancer (Nes-GFP$^+$ cells) [16] are multipotent, display *in vivo* self-renewal and support the maintenance of hematopoietic stem cells, suggesting that Nes-GFP identifies SSCs in the adult bone marrow compartment [17]. During the endochondral ossification process in bone development, Nes-GFP$^+$ cells are abundant in the perichondrium and are characterized as early cells in the osteoblast as well as endothelial lineage [18]. The properties of Nes-GFP$^+$ cells in adult mouse periosteum however remain poorly described, and their role during fracture healing unknown.

In this study, we investigated whether the Nes-GFP transgene marks SSCs in the periosteum. We show that Nes-GFP$^+$ cells are present in the periosteum at a perivascular localization and that they express other SSC and progenitor markers, although at a different level compared to Nes-GFP$^+$ cells in the bone marrow. Our data suggest that, in the periosteum, Nes-GFP is primarily expressed by a population of skeletal progenitors that strongly proliferate and contribute to the osteoblast pool during bone regeneration.

2. Materials and methods

2.1. Animals and cell isolation

Nestin-GFP (Nes-GFP) transgenic mice (C57/BL6 background)[16] were kindly provided by Dr Grigori Enikolopov at Cold Spring Harbor Laboratory. The mice were housed in conventional conditions in our animal housing facility (Proefdierencentrum Leuven, Belgium) at 22°C under a 14-hour light/10-hour dark cycle, fed a normal chow diet (V1535; Ssniff GmbH, Soest, Germany) and analyzed at 8 weeks of age. Previous bone-healing studies from our laboratory did not find sex-specific differences and we therefore used both male and female mice. All animal experiments were conducted according to the regulations and with approval of the Animal Ethics Committee of the KU Leuven.

Murine periosteum-derived cells (mPDC), flushed bone marrow cells (mBMC-F) and bone marrow cells digested from bone fragments (mBMC-B) were isolated from Nes-GFP mice [19]. Briefly, the tibiae and femora were dissected and the muscles removed. The epiphyses were embedded in 5% low melting point agarose (SeaPlaque; Lonza, Verviers, Belgium). Periosteal cells were obtained by sequential digestion with a mixture of 3mg/ml collagenase and 4mg/ml dispase in Minimum Essential Media (MEM) α medium (all from Gibco; Life Technologies, Ghent, Belgium). Cells obtained after 10 minutes of digest were discarded. The cells obtained during the second digest (50 minutes) were passed through a 70 µm nylon mesh and used for further analysis. To collect the mBMC-F fraction, the epiphyses were removed and the bone marrow was flushed out with 0.5 mL of phosphate-buffered saline (PBS) using a syringe with 26G needle. Finally, the mBMC-B fraction was obtained by crushing of the remaining bone and digesting the bone fragments with the collagenase/dispase mixture.

2.2. Flow Cytometry Analysis and cell sorting

Freshly isolated mPDC, mBMC-F and mBMC-B were resuspended in PBS supplemented with 2% fetal bovine serum (FBS; Gibco) and 2mM EDTA. The cells were incubated for 30 min at 4°C

with the respective antibodies at the indicated concentration (Table 1). Flow cytometry analysis was performed on a Gallios Flow Cytometer (Beckman Coulter, Brea, USA) and analyzed by using the Kaluza software (Beckman Coulter). Due to the high amount of hematopoietic cells in the bone marrow fraction, a Lineage Cell Depletion Kit and CD45 MicroBeads were used together with LD columns (all from Miltenyi biotech, Bergisch Gladbach, Germany) according to manufacturer's instructions before investigating the panels of markers described in Chan et al. 2015 [12].

To obtain Nes-GFP$^+$ cells from the periosteum, mPDC from Nes-GFP$^+$ mice were isolated and incubated with Ter119-APC, CD45-APC and CD31-APC antibodies (eBioscience; Thermo Fisher Scientific, Asse, Belgium). The Nes-GFP$^-$ and Nes-GFP$^+$ cells in the Ter119$^-$CD45$^-$CD31$^-$ population were then sorted by flow cytometry (BD FACSAria III, BD Biosciences, Erembodegem, Belgium).

2.3. Mouse models

To determine whether Nes-GFP$^+$ cells are slow dividing cells, Nes-GFP$^+$ mice received 5-Iodo-2′-deoxyuridine (IdU) (1mg/mL; Sigma-Aldrich, Diegem, Belgium) in their drinking water for 30 days followed by a chase period of 40 days with normal drinking water.

For the fracture model, an osteotomy was used to mimic a simple transverse fracture pattern. Mice were anesthetized by peritoneal injection of a ketamine-xylazine mixture in saline (ketamine at 100 mg/kg and xylazine at 15 mg/kg). The right leg was shaved, disinfected and the tibia was exposed. A fracture was made with a diamond saw, taking care not to damage the underlying muscle tissue. The fibula was cut and the tibia fracture was immobilized by introducing from the knee joint a 26G needle into the bone marrow canal. The skin was then sutured and analgesics administered by peritoneal injection (Temgesic diluted 1/50 in saline at 10mg/kg). After 1, 3 or 7 days, BrdU in saline (150 mg/kg BW; Sigma-Aldrich, Diegem, Belgium)

was delivered by peritoneal injection 4h prior to sacrifice. The mice were then anesthetized and perfused with heparinized PBS followed by 2% paraformaldehyde in PBS.

For the kidney capsule implantation, Nes-GFP$^+$ were sorted by flow cytometry and resuspended in matrigel (Corning GmbH, Wiesbaden, Germany) at a concentration of 1000 cells/µL. 2µL of matrigel was then injected underneath the renal capsule of 8 week old C57/Bl6 mice. After 8 weeks recipient mice were euthanized, the kidney retrieved and fixed in 2% paraformaldehyde in PBS.

2.4. Bone formation by Ex Vivo micro–computed tomography (µCT)

Upon sample retrieval and fixation in 2% paraformaldehyde in PBS, the presence of mineralized tissues in the kidney was assessed by µCT analysis using a SkyScan 1172 µCT system (Bruker, Kontich, Belgium) at a pixel size of 5µm with 50kV tube voltage and 0.5mm aluminium filter. Reconstruction was performed with NRecon software (Bruker).

2.5. (Immuno)histochemistry

Isolated tibiae and kidneys were fixed overnight in 2% paraformaldehyde and decalcified in EDTA (0,5M; pH 7,5) for 14 days at 4°C. For the fracture experiments, bones were embedded in NEG-50 frozen section medium (Richard-Allen Scientific, Thermo Fisher Scientific), and sectioned with a cryostat at 7 µm using the CryoJane system. Kidneys with transplanted cells were processed in the same way. The bones of the mice that received IdU in their drinking water were embedded in paraffin and sectioned at 4 µm. Hematoxylin and eosin (H&E) and immunohistochemical stainings are routinely performed in our lab as described previously [20–22]. The antibodies used in these experiments are listed in Table 1. Images were taken on a Zeiss Axioplan 2 light microscope (Carl Zeiss Microscopy GmbH, Jena, Germany). The quantification of cells that are double positive for BrdU/NesGFP, Osx/NesGFP or IdU/NesGFP

as well as of the proportion of NesGFP$^+$ cells that are located next to blood vessels was performed by using the ImageJ software (NIH, Bethesda, MD, USA; https://imagej.nih.gov/ij/).

Table 1: List of antibodies used for immunofluorescence and flow cytometry analysis.

	Antigen/reagent	Host/Isotype	Conjugate	Supplier	Catalog number	Dilution
Primary antibodies	BP1	Rat / IgG2a	PE	eBioscience	12-5891-81	1/200
	BrdU	Rat / IgG2a	-	Serotec	OBT0030	1/100
	CD31	Rat / IgG2a	-	BD Biosciences	550274	1/100
	CD31	Rat / IgG2a	APC	eBioscience	17-0311-80	1/500
	CD45	Rat / IgG2b	APC	eBioscience	17-0451-83	1/500
	CD51	Rat / IgG1	PE	eBioscience	12-0512-81	1/40
	CD51	Rat / IgG1	Biotin	eBioscience	13-0512-82	1/200
	CD90.2	Rat / IgG2b	PE	eBioscience	12-0903-81	1/200
	CD105	Rat / IgG2a	Pacific Blue	Biolegend	120412	1/200
	CD105	Rat / IgG2a	PE	eBioscience	12-1051-81	1/40
	CD200	Rat / IgG2a	PerCP-eFluor 710	eBioscience	46-5200-82	1/200
	GFP	Rabbit / IgG	-	Invitrogen	A11122	1/200
	IdU	Mouse / IgG1	-	Abcam	ab8955	1/250
	Leptin receptor	Goat / IgG	Biotin	R&D Systems	BAF497	1/50
	Osterix	Rabbit / IgG	-	Santa Cruz	sc-22536-R	1/10000
	PDGFR-α	Rat / IgG2a	PE	eBioscience	12-1401-81	1/50
	Sca-1	Rat / IgG2a	PE	eBioscience	12-5981-82	1/200
	SOX9	Rabbit / IgG	-	Novus	NBP1-85551	1/100
	Ter119	Rat / IgG2b	APC	eBioscience	17-5921-83	1/200
Secondary antibodies / amplification kits	anti-mouse	Goat / IgG	Alexa546	Life Technologies	A11003	1/100
	anti-rabbit	Goat / IgG	Alexa488	Life Technologies	A11008	1/200
	anti-rabbit	Goat / IgG	Alexa546	Life Technologies	A11010	1/200
	anti-rat	Goat / IgG	Alexa568	Life Technologies	A11077	1/500
	Streptavidin	-	PE-Cyanine7	eBioscience	25-4317-82	1/200
	Streptavidin	-	PE	eBioscience	12-4317-87	1/200
	TSA fluorescein system	-	-	Perkin Elmer	NEL701001KT	-
	TSA Cyanine 3 system	-	-	Perkin Elmer	NEL704A001KT	-

2.6. Cell cultures

For the *in vitro* fibroblastic colony-forming unit (CFU-F) assay, sorted mPDC were seeded at very low density (10 cells/cm^2) in Dulbecco's Modified Eagle Medium (DMEM) with 25mM of glucose and containing 15% FBS and 2 mM Glutamine (all from Gibco). After 10 days, the colonies were fixed with a solution of periodate-lysine-paraformaldehyde, stained with methylene blue (Sigma-Aldrich, Diegem, Belgium) and the number of colonies containing at least 20 cells was quantified.

For the *in vitro* differentiation assays, colonies cultured for 10 days in normal medium were switched to specific differentiation medium for additional 10 days: for osteogenic differentiation medium was supplemented with 10 mM β-glycerophosphate and 50 µg/ml L-ascorbic acid (both from Sigma-Aldrich); for chondrogenic differentiation 10 ng/ml recombinant human transforming growth factor-β 1 (Peprotech, Rocky Hill, CT, USA), 50 µg/ml L-ascorbic acid and 20µM Y-27632 (ROCK inhibitor, Axon Medchem, Groningen, The Netherlands) were added and for adipogenic differentiation 10nM Dexamethasone, 50µM Indomethacin, 10µg/mL Insulin and 500nM IBMX (all from Sigma-Aldrich) were added. After the differentiation period, colonies were stained respectively for Alkaline phosphatase activity (ALP), glycosaminoglycans (Alcian Blue 8GX; 1% in 0.1 N HCl; pH 1.2; Sigma-Aldrich) and lipid droplets (Oil Red O; Sigma-Aldrich) [19].

2.7. RNA extraction and quantitative real-time (qRT)-PCR analysis

RNA from differentiated and undifferentiated colonies was extracted using the Nucleospin RNA isolation Kit (Macherey-Nagel GmbH, Duren, Germany) according to the manufacturer's instructions. Reverse transcription was performed using the Superscript II Reverse Transcriptase (Invitrogen, Thermo Fisher Scientific) and the analysis of quantitative reverse transcriptase polymerase chain reaction (qRT-PCR) was performed on the StepOnePlus Real-Time PCR System (Applied Biosystems, Thermo Fisher Scientific) using specific forward and reverse oligonucleotide primers as well as probes with fluorescent dye (FAM) and quencher (TAMRA) (Supporting Information Table 2). Expression levels were normalized for the expression of the housekeeping gene hypoxanthine-guanine phosphoribosyl transferase (*mHprt*) by using the ΔΔCT method.

Table 2: Mouse primer sequences of target genes.

gene	forward primer	probe	reverse primer
Alp	CGCACGCGATGCAACA	CACTCAGGGCAATGAGGTCACATCCA	CGGACTTCCCAGCATCCTT
Coll1	TGTCCCAACCCCCAAAGAC	ACGTATTCTTCCGGGCAGAAAGCACA	CCCTCGACTCCTACATCTTCTGA
Coll2	AGAACATCACCTACCACTGTAAGAACA	CCTTGCTCATCCAGGGCTCCAATG	TGACGGTCTTGCCCCACTT
Pparg	CCCAATGGTTGCTGATTACAAA	CTGAAGCTCCAAGAATACCAAAGTGCGATC	AATAATAAGGTGGAGATGCAGGTTCT
Sox9	TCTGGAGGCTGCTGAACGA	CAGCACAAGAAAGACCACCC	TCCGTTCTTCACCGACTTCCT

2.8. Statistical analysis

Data are presented as mean ± SD and analyzed by Student's t-test or ANOVA as indicated in the figures. n values represent the number of individual mice or pools of cells that have been studied. Differences were considered statistically significant at $p<0.05$.

2.9 Figure art

Schematics included in the figures were created using Servier Medical Art templates, which are licensed under a Creative Commons Attribution 3.0 Unported License; https://smart.servier.com.

3. Results

3.1. Mouse periosteal and bone marrow-derived Nes-GFP$^+$ cells differ in stem cell marker expression

In contrast to the thorough characterization of bone marrow skeletal stem cells (SSCs), knowledge on periosteal SSCs is only emerging recently. The Nes-GFP transgene has been described to label SSCs in the bone marrow [17] and we therefore investigated whether Nes-GFP can also be used to mark periosteal SSCs. Histological analysis of adult mouse tibia showed that Nes-GFP$^+$ cells are detected in the periosteum and 73±9% of Nes-GFP$^+$ cells was localized in close proximity to blood vessels (Figure 1A). We next analyzed what the proportion is of Nes-GFP$^+$ cells in the stromal fraction of the periosteum (mPDC) in comparison to their percentage in the stromal fraction of the flushed bone marrow (mBMC-F) or after digestion of the bone fragments (mBMC-B). Flow cytometry analysis showed that almost 37.7±4.3% of the total mPDC population were stromal cells (Ter119$^-$CD45$^-$CD31$^-$), whereas stromal cells were scarce in the two bone marrow fractions (1.3±0.3 and 4.4±0.6% in respectively mBMC-F and mBMC-B; Figure 1B). Nes-GFP$^+$ cells were more abundant in the total mPDC population (6.5±1.8%) versus bone marrow populations (0.006±0.002 and 0.10±0.08% in respectively mBMC-F and mBMC-B; Figure 1C), as well as in the stromal fraction of the periosteum (17.3±4.8%) compared to the bone marrow (1.3±0.2%; Figure 1D). We also noticed that the expression of other markers that are reported to label stem cells and/or progenitors differed between these two cell sources, with more Sca1$^+$ cells, but less CD105$^+$ and PDGFRα^+ cells in periosteum compared to bone marrow (Figure 1D). Cells expressing LepR or CD51 were equally abundant in periosteal and bone marrow stromal fractions. In addition, the expression of these stem cell and progenitor markers by Nes-GFP$^+$ cells depended on their origin, with fewer periosteal Nes-GFP$^+$ cells expressing LepR or PDGFRα, but more periosteal Nes-GFP$^+$ cells expressing Sca1 compared to bone marrow Nes-GFP$^+$ cells (Figure 1E). Taken together, Nes-GFP$^+$ cells are present in the

periosteum at a perivascular location, but they differ in the expression of stem cell and progenitor markers from Nes-GFP$^+$ cells in the bone marrow.

3.2. Nes-GFP labels skeletal progenitors in the periosteum

In order to determine whether periosteal Nes-GFP$^+$ cells are SSCs, we first investigated whether they are slow-dividing cells, a characteristic of many stem cells [23–27]. To this end, the thymidine analogue (IdU) was added to the drinking water during 30 days to 8-week-old mice. Histological analysis showed that 27.2±11.8% (n=3; mean ± SD) of the Nes-GFP$^+$ cells in the periosteum were labeled by IdU, indicating that these cells have divided at least once during this period (Figure 2A). Next, mice received normal drinking water during 40 days, which will result in loss of IdU in proliferating cells whereas the slow-dividing cells will still contain IdU [24,28]. We could not detect IdU$^+$ Nes-GFP$^+$ double positive cells following the chase period of 40 days, indicating that periosteal Nes-GFP$^+$ cells do not exhibit the slow-dividing property of SSCs (Figure 2A).

Next, we investigated the *in vitro* colony forming and trilineage differentiation capacity of sorted periosteal Ter119$^-$CD45$^-$CD31$^-$Nes-GFP$^+$ cells, known characteristics of SSCs. Nes-GFP$^+$ cells were able to form both primary and secondary colonies, but the colony forming efficiency was comparable to the Nes-GFP$^-$ fraction (Figures 2B-C). Furthermore, the colonies formed by Nes-GFP$^+$ and Nes-GFP$^-$ cells had a comparable capacity to differentiate along the osteogenic, chondrogenic and adipogenic lineage, as evidenced by respectively ALP staining and *Alp* and *Col1* expression (Figure 2D-F), Alcian Blue staining and *Sox9* and *Col2* expression (Figure 2G-I) and Oil red O staining and *Ppar*γ expression (Figure 2J, 2K).

In their study, Chan et al. 2015 [12] described panels of markers that label SSCs (Ter119$^-$CD45$^-$CD31$^-$CD51$^+$CD90$^-$BP1$^-$CD105$^-$CD200$^+$), pre-Bone Cartilage and Stromal Progenitors (pre-

BCSPs; Ter119$^-$CD45$^-$CD31$^-$CD51$^+$CD90$^-$BP1$^-$CD105$^-$CD200$^-$) and Bone, Cartilage, and Stromal Progenitors (BCSPs; Ter119$^-$CD45$^-$CD31$^-$CD51$^+$CD90$^-$BP1$^-$CD105$^+$CD200$^-$). These three populations have been described to be multipotent cells that form bone, cartilage and marrow after *in vivo* implantation. We investigated if Nes-GFP$^+$ expression overlaps with these three populations in periosteum and bone marrow. Of the periosteal Nes-GFP$^+$ stromal cells, less than 5% are immunophenotypic SSCs, about 14% are pre-BCSPs and 8% are BCSPs (Figure 3A). In contrast, more than half of the Nes-GFP$^+$ stromal cells in the bone marrow have the cell surface marker profile of SSCs, about 7% that of pre-BCSPs and only less than 2% that of BCSPs (Figure 3B). Altogether, the SSC/pre-BCSP/BCSP cells are 26.6±3.1% (n=4; mean ± SD) (Figure 3A) of Nes-GFP$^+$ stromal cells in the periosteum versus 61±3.2% (n=4; mean ± SD) in bone marrow (Figure 3B). We further tested the properties of periosteal Nes-GFP$^+$ cells *in vivo* by sorting and transplanting these cells under the kidney capsule in wildtype recipient mice. The kidney capsule provides an environment rich in blood vessels and nutrients that promotes survival and growth of implanted cells [29,30]. True SSCs, but also pre-BCSPs and BCSPs, will form bone, cartilage and hematopoiesis-supportive stroma in this model [11]. We retrieved the kidneys and implanted cells after 8 weeks and assessed the presence of mineralized tissue by µCT analysis. Mineralized tissue was found in 4 out of the 12 samples (Figure 3C), which was confirmed to be bone tissue by histological analysis (Figure 3D). However, no cartilage or hematopoietic tissue was observed. In addition, no Nes-GFP$^+$ cells were found in any of the transplants (Figure 3E). However, the Nes-GFP transgene does not allow to trace the progeny of the implanted cells as its expression is lost upon differentiation. Therefore, these data show that Nes-GFP$^+$ periosteal cells have the *in vivo* potency to form bone, but they are not self-renewing SSCs. These findings are in line with our flow cytometry analysis showing that the proportions of SSCs, pre-BCSPs and BCSPs are low in the periosteal Nes-GFP$^+$ cell pool.

Together, these data indicate that periosteal Nes-GFP$^+$ cells are not true SSCs but rather display properties of skeletal progenitors.

3.3. Periosteal Nes-GFP$^+$ cells proliferate and contribute to the osteoblast pool in response to fracture

Skeletal stem and progenitor cells drive bone regeneration by proliferating and subsequently differentiating to chondrocytes or osteoblasts. Since our data show that periosteal Nes-GFP$^+$ cells are skeletal progenitor cells, we investigated the behavior of Nes-GFP$^+$ cells during the early phases of bone healing, at 1, 3 and 7 days after fracture of the tibia in mice (Figure 4A). These time points correspond respectively to the inflammatory phase, the thickening of the periosteum with increased proliferation of skeletal cells and the formation of the soft callus consisting of cartilage and immature bone tissue. (Figure 4B). First, to assess proliferation, mice were injected with BrdU 4h before sacrifice (Figure 4A) and the percentage of proliferative (BrdU$^+$) Nes-GFP$^+$ cells was quantified in a pre-defined region of the periosteum close to the fracture site (boxed area in Figure 4B). Of note, BrdU$^+$ cells were not detected in the periosteum of a non-fractured tibia (Figure 4C). One day after fracture, 15.2±5.9% of Nes-GFP$^+$ cells were BrdU$^+$ and this proportion increased up to 24.9±2.5% at day 3 and then decreased again to 16.5±3% at day 7 (Figure 4C-D). In accordance, the total number of Nes-GFP$^+$ cells per callus area increased from 4.8±0.8 at day 1 to 20.4±11.8 and 60.5±24.5 at respectively day 3 and 7 after fracture (n=4; mean ± SD). These data show that Nes-GFP$^+$ cells contribute substantially to the proliferative response of the periosteum after fracture, with a peak of proliferation detected 3 days after the fracture.

We then investigated whether the location of Nes-GFP$^+$ cells in the periosteum changed after fracture. As mentioned, the majority of Nes-GFP$^+$ cells localize close to blood vessels in unstressed conditions (Figure 1A) and this presence of Nes-GFP$^+$ cells in direct contact with CD31$^+$ cells remained similar at day 1, 3 and 7 after fracture (Figure 4E-F). Thus, most Nes-GFP$^+$ cells stay in a perivascular location during the process of bone repair.

Finally, we investigated whether periosteal Nes-GFP$^+$ cells exhibit properties of chondro- or osteoprogenitors by analyzing whether Nes-GFP$^+$ cells express respectively Sox9 or Osterix (Osx) 7 days after fracture (Figure 4G-H). Cells expressing both Nes-GFP and Sox9 were not detected, but Nes-GFP$^+$/Osx$^+$ cells were observed, confirming the notion that Nes-GFP labels osteoprogenitors in the periosteum. The proportion of Nes-GFP$^+$ cells that expressed Osx did not change significantly after fracture, ranging from 15.2±2.7% in unfractured periosteum to 8.8±4.2% at day 7 after fracture (n=3; mean ± SD). Conversely, 5±0.6% of the Osx$^+$ cell population was positive for Nes-GFP (n=3; mean ± SD), and this fraction was not different from the unfractured condition (9.3±5.7%; n=3; mean ± SD). Thus, while the total number of Nes-GFP$^+$ cells increases during the early phases of fracture healing in mice, the percentage of Nes-GFP$^+$ cells committed to the osteogenic lineage does not change. These data reveal that also during fracture healing periosteal Nes-GFP$^+$ cells behave like osteoprogenitor cells, showing a strong proliferative response and contributing to the osteoprogenitor pool.

4. Discussion

The periosteum has a critical role during bone repair [4,5], but consists of a heterogenous pool of cells, including SSCs. To better understand periosteal biology and optimize the therapeutic potential of stem cell strategies for bone regeneration [31–33], cell markers that identify periosteal SSCs are needed. Since Nes-GFP labels SSCs in the bone marrow, we questioned whether this marker also identifies SSCs in the periosteum. We here report that Nes-GFP labels osteolineage-restricted skeletal progenitors in the adult mouse periosteum rather than true SSCs, and that these cells proliferate during bone fracture healing.

Similar to Nes-GFP$^+$ cells in the bone marrow [17], we found that periosteal Nes-GFP$^+$ cells localize primarily perivascular. However, Nes-GFP$^+$ cells in these two compartments differed in most other characteristics. First, the number of Nes-GFP$^+$ cells in the stromal fraction of the periosteum is much higher compared to the bone marrow. Second, periosteal Nes-GFP$^+$ cells express stem cell and progenitor markers at different levels compared to those in the bone marrow, with lower expression of LepR and of PDGFRα, but higher expression of Sca1. The differences between Nes-GFP$^+$ cells from these two cell sources is further underscored by our flow cytometry analysis using the markers first described by Chan *et al*. [12]. Indeed, periosteal Nes-GFP$^+$ contain much less multipotent cells compared to bone marrow Nes-GFP$^+$ cells, and the proportion of SSCs is less than 5% of Nes-GFP$^+$ cells in periosteum versus more than half of Nes-GFP$^+$ cells in the bone marrow. Our findings differ from recently reported data, which show a much lower abundance of Nes-GFP$^+$ cells in the periosteum (0.64% of total pool vs 6.5% in our study) and a higher expression level of PDGFRα [34]. A possible explanation is the different method of isolation of mPDC, where Gao et al. used mechanical dissection of the periosteum followed by an enzymatic digestion, whereas we only used a histologically validated enzymatic digestion [19]. *In vitro* testing of the properties of periosteal Nes-GFP$^+$ cells revealed that these cells can form both primary and secondary fibroblastic colonies and exhibit trilineage

differentiation potential, both characteristics that are often used as a proxy for the presence of SSCs. However, the same *in vitro* SSC properties were found in periosteal Nes-GFP$^-$ cells. Our subsequent *in vivo* analyses revealed that Nes-GFP$^+$ periosteal cells derived from 8 week-old mice are not slow dividing, do not renew themselves and give rise to only bone tissue after transplantation, thus showing the characteristics of osteoprogenitor cells rather than SSCs. Again, periosteal Nes-GFP$^+$ cells differ from the ones in the bone marrow compartment which show *in vivo* self-renewal and multipotency when seeded on ceramic carriers and implanted under the skin in mice [17]. Although a different model was used to investigate the *in vivo* properties of periosteal Nes-GFP$^+$ cells in our study, the high proportions of SSCs, pre-BCSPs and BCSPs in bone marrow Nes-GFP$^+$ cells suggest potential self-renewal and multipotency also in the kidney capsule model [12]. These results again highlight the risk of relying solely on *in vitro* assays, and underscore the importance of performing adequate *in vivo* assays to assess stem cell properties, as has been advocated before [1]. Interestingly, Nes-GFP does seem to label self-renewing SSCs in the mouse periosteum during bone development, but the number of Nes-GFP$^+$ periosteal cells decreases with age [34]. Together with our current results, these data show that the periosteal SSC subset marked by the Nes-GFP transgene during development is lost in adulthood. While it is clear that SSCs exist in the adult mouse periosteum, as recently evidenced by serial transplantation and fracture experiments [6], markers to readily isolate these cells remain elusive. One interesting tool is the LepR-cre mouse line, which labels SSCs in the adult mouse periosteum [9,34], but the constitutive nature of this transgene makes it unclear whether adult periosteal SSCs still express LepR and could be isolated using an antibody-based approach. A recent study used the cathepsin K-cre mouse line in combination with a panel of cell surface markers to identify periosteal skeletal stem cells [35], providing for the first time a promising approach to specifically identify and isolate periosteal SSCs.

While they may not be true SSCs, periosteal Nes-GFP$^+$ cells in adult mice do play a role in the bone healing process, as they start to proliferate after fracture and contribute to Osx$^+$ osteogenic cells in the callus. It is unclear whether all osteoblasts in the fracture callus are derived from Nes-GFP$^+$ progenitors or only a fraction, since the nature of the Nes-GFP transgene does not allow lineage tracing. We did find that none of the Nes-GFP$^+$ cells express the early chondrogenic marker Sox9 after fracture, making it likely that Nes-GFP$^+$ periosteal cells are restricted to the osteogenic lineage also during bone healing. Given that nearly all osteoblasts in a fracture callus are marked by LepR-cre [9], the Nes-GFP$^+$ fraction may represent an intermediate osteoprogenitor cell state that derives from SSC marked by LepR-cre and gives itself rise to Osx$^+$ preosteoblasts. It is important to note that the skeleton of 8 week old mice, as used in this study, is still growing [36,37]. Therefore, it is possible that murine periosteal Nes-GFP$^+$ cells may undergo further changes with skeletal maturation.

Overall, our study highlights important differences between periosteal and bone marrow cells with regards to cell identity markers, and urges caution in translating markers between the two cell sources. The Nes-GFP transgene, while marking SSCs in the adult mouse bone marrow and developing periosteum, labels adult mouse periosteal skeletal progenitors, but not SSCs.

Author's contribution

G.T., G.C. and N.v.G. conceptualized and designed the study, G.T., S.S., G.G., I.S., K.M. and N.v.G. acquired data. G.T., G.C. and N.v.G. performed analysis and interpretation of the data. G.T., G.C. and N.v.G. wrote the manuscript.

Acknowledgements

The authors wish to thank Riet Van Looveren and Sophie Torrekens for technical assistance. G.C. acknowledges funding from Fund for Scientific Research-Flanders (FWO: G.0A42.16 and G.0B3418) and from KUL (C24/17/077). N.v.G. was funded by BOF-KU Leuven GOA project 3M120209. S.S. is a postdoctoral fellow from the FWO (12H5917N).

The authors declare no conflict of interest.

Reference List

[1] P. Bianco, X. Cao, P.S. Frenette, J.J. Mao, P.G. Robey, P.J. Simmons, C.-Y. Wang, The meaning, the sense and the significance: translating the science of mesenchymal stem cells into medicine., Nat. Med. 19 (2013) 35–42. doi:10.1038/nm.3028.

[2] B. Sacchetti, A. Funari, S. Michienzi, S. Di Cesare, S. Piersanti, I. Saggio, E. Tagliafico, S. Ferrari, P.G. Robey, M. Riminucci, P. Bianco, Self-Renewing Osteoprogenitors in Bone Marrow Sinusoids Can Organize a Hematopoietic Microenvironment, Cell. 131 (2007) 324–336. doi:10.1016/j.cell.2007.08.025.

[3] A.J. Friedenstein, R.K. Chailakhyan, N. V. Latsinik, A.F. Panasyvk, I. V. Keiliss-Borok, Stromal cells responsible for transferring the microenvironment of the hemopoietic tissues: Cloning in vitro and retransplantation in vivo, Transplantation.17 (1974) 331-40. doi:10.1097/00007890-197404000-00001.

[4] C. Colnot, Skeletal cell fate decisions within periosteum and bone marrow during bone regeneration., J. Bone Miner. Res. 24 (2009) 274–82. doi:10.1359/jbmr.081003.

[5] X. Zhang, C. Xie, A.S.P. Lin, H. Ito, H. Awad, J.R. Lieberman, P.T. Rubery, E.M. Schwarz, R.J. O'Keefe, R.E. Guldberg, Periosteal progenitor cell fate in segmental cortical bone graft transplantations: implications for functional tissue engineering., J. Bone Miner. Res. 20 (2005) 2124–37. doi:10.1359/JBMR.050806.

[6] O. Duchamp De Lageneste, A. Julien, R. Abou-Khalil, G. Frangi, C. Carvalho, N. Cagnard, C. Cordier, S.J. Conway, C. Colnot, Periosteum contains skeletal stem cells with high bone regenerative potential controlled by Periostin, Nat. Commun. 9 (2018) 773. doi:10.1038/s41467-018-03124-z.

[7] C. De Bari, F. Dell'Accio, J. Vanlauwe, J. Eyckmans, I.M. Khan, C.W. Archer, E.A. Jones, D. McGonagle, T.A. Mitsiadis, C. Pitzalis, F.P. Luyten, Mesenchymal multipotency of adult human periosteal cells demonstrated by single-cell lineage analysis, Arthritis Rheum. 54 (2006) 1209–1221. doi:10.1002/art.21753.

[8] N. Van Gastel, S. Stegen, I. Stockmans, K. Moermans, J. Schrooten, D. Graf, F.P. Luyten, G. Carmeliet, Expansion of murine periosteal progenitor cells with fibroblast growth factor 2 reveals an intrinsic endochondral ossification program mediated by bone morphogenetic protein 2, Stem Cells. 32 (2014) 2407–2418. doi:10.1002/stem.1783.

[9] B.O. Zhou, R. Yue, M.M. Murphy, J.G. Peyer, S.J. Morrison, Leptin-receptor-expressing mesenchymal stromal cells represent the main source of bone formed by adult bone marrow, Cell Stem Cell. 15 (2014) 154-68. doi:10.1016/j.stem.2014.06.008.

[10] C.K.F. Chan, P. Lindau, W. Jiang, J.Y. Chen, L.F. Zhang, C.-C. Chen, J. Seita, D. Sahoo, J.-B. Kim, A. Lee, S. Park, D. Nag, Y. Gong, S. Kulkarni, C.A. Luppen, A.A. Theologis, D.C. Wan, A. DeBoer, E.Y. Seo, J.D. Vincent-Tompkins, K. Loh, G.G. Walmsley, D.L. Kraft, J.C. Wu, M.T. Longaker, I.L. Weissman, Clonal precursor of bone, cartilage, and hematopoietic niche stromal cells, Proc. Natl. Acad. Sci. 110 (2013) 12643-8.doi:10.1073/pnas.1310212110.

[11] O. Marecic, R. Tevlin, A. McArdle, E.Y. Seo, T. Wearda, C. Duldulao, G.G. Walmsley, A. Nguyen, I.L. Weissman, C.K.F. Chan, M.T. Longaker, Identification and characterization of an injury-induced skeletal progenitor, Proc. Natl. Acad. Sci. 112 (2015) 9920-5. doi:10.1073/pnas.1513066112.

[12] C.K.F. Chan, E.Y. Seo, J.Y. Chen, D. Lo, A. McArdle, R. Sinha, R. Tevlin, J. Seita, J. Vincent-Tompkins, T. Wearda, W.J. Lu, K. Senarath-Yapa, M.T. Chung, O. Marecic, M. Tran, K.S. Yan, R. Upton, G.G. Walmsley, A.S. Lee, D. Sahoo, C.J. Kuo, I.L. Weissman, M.T. Longaker, Identification and specification of the mouse skeletal stem cell, Cell. 160 (2015) 285-98. doi:10.1016/j.cell.2014.12.002.

[13] S. Morikawa, Y. Mabuchi, Y. Kubota, Y. Nagai, K. Niibe, E. Hiratsu, S. Suzuki, C. Miyauchi-Hara, N. Nagoshi, T. Sunabori, S. Shimmura, A. Miyawaki, T. Nakagawa, T. Suda, H. Okano, Y. Matsuzaki, Prospective identification, isolation, and systemic transplantation of multipotent mesenchymal stem cells in murine bone marrow, J. Exp. Med. 206 (2009) 2483-96. doi:10.1084/jem.20091046.

[14] D.D. Houlihan, Y. Mabuchi, S. Morikawa, K. Niibe, D. Araki, S. Suzuki, H. Okano, Y. Matsuzaki, Isolation of mouse mesenchymal stem cells on the basis of expression of Sca-1 and PDGFR-α, Nat. Protoc. 7 (2012) 2103-11. doi:10.1038/nprot.2012.125.

[15] A. Bernal, L. Arranz, Nestin-expressing progenitor cells: function, identity and therapeutic implications, Cell. Mol. Life Sci. 75 (2018) 2177-2195. doi:10.1007/s00018-018-2794-z.

[16] J.L. Mignone, V. Kukekov, A.S. Chiang, D. Steindler, G. Enikolopov, Neural Stem and Progenitor Cells in Nestin-GFP Transgenic Mice, J. Comp. Neurol. 469 (2004) 311-24. doi:10.1002/cne.10964.

[17] S. Méndez-Ferrer, T. V. Michurina, F. Ferraro, A.R. Mazloom, B.D. MacArthur, S.A. Lira, D.T. Scadden, A. Mag'Ayan, G.N. Enikolopov, P.S. Frenette, Mesenchymal and haematopoietic stem cells form a unique bone marrow niche, Nature. 466 (2010) 829-34. doi:10.1038/nature09262.

[18] N. Ono, W. Ono, T. Mizoguchi, T. Nagasawa, P.S. Frenette, H.M. Kronenberg, Vasculature-associated cells expressing nestin in developing bones encompass early cells in the osteoblast and endothelial lineage, Dev. Cell. 29 (2014) 330-9. doi:10.1016/j.devcel.2014.03.014.

[19] N. Van Gastel, S. Torrekens, S.J. Roberts, K. Moermans, J. Schrooten, P. Carmeliet, A. Luttun, F.P. Luyten, G. Carmeliet, Engineering vascularized bone: Osteogenic and proangiogenic potential of murine periosteal cells, Stem Cells. 30 (2012) 2460–2471. doi:10.1002/stem.1210.

[20] S. Stegen, N. Van Gastel, G. Eelen, B. Ghesquière, F. D'Anna, B. Thienpont, J. Goveia, S. Torrekens, R. Van Looveren, F.P. Luyten, P.H. Maxwell, B. Wielockx, D. Lambrechts, S.M. Fendt, P. Carmeliet, G. Carmeliet, HIF-1α promotes glutamine-mediated redox homeostasis and glycogen-dependent bioenergetics to support postimplantation bone cell

survival, Cell Metab. 23 (2016) 265–279. doi:10.1016/j.cmet.2016.01.002.
[21] S. Stegen, K. Laperre, G. Eelen, G. Rinaldi, P. Fraisl, S. Torrekens, R. Van Looveren, S. Loopmans, G. Bultynck, S. Vinckier, F. Meersman, P.H. Maxwell, J. Rai, M.A. Weis, D.R. Eyre, B. Ghesquière, S.M. Fendt, P. Carmeliet, G. Carmeliet, HIF-1α metabolically controls collagen synthesis and modification in chondrocytes, Nature. 565 (2019) 511-515. doi:10.1038/s41586-019-0874-3.
[22] P.J. Stiers, S. Stegen, N. van Gastel, R. Van Looveren, S. Torrekens, G. Carmeliet, Inhibition of the Oxygen Sensor PHD2 Enhances Tissue-Engineered Endochondral Bone Formation, J. Bone Miner. Res. 34 (2019) 333-348. doi:10.1002/jbmr.3599.
[23] J.M. Bernitz, H.S. Kim, B. MacArthur, H. Sieburg, K. Moore, Hematopoietic Stem Cells Count and Remember Self-Renewal Divisions, Cell. 167 (2016) 1296-1309. doi:10.1016/j.cell.2016.10.022.
[24] M. Kimoto, Y. Yura, M. Kishino, S. Toyosawa, Y. Ogawa, Label-retaining cells in the rat submandibular gland, J. Histochem. Cytochem. 56 (2008) 15-24. doi:10.1369/jhc.7A7269.2007.
[25] Y. Li, K. Watanabe, M. Fujioka, K. Ogawa, Characterization of slow-cycling cells in the mouse cochlear lateral wall, PLoS One. 12 (2017) e0179293. doi:10.1371/journal.pone.0179293.
[26] R.J. Morris, C.S. Potten, Slowly cycling (label-retaining) epidermal cells behave like clonogenic stem cells in vitro, Cell Prolif. 27 (1994) 279-89. doi:10.1111/j.1365-2184.1994.tb01425.x.
[27] J.A. Oliver, O. Maarouf, F.H. Cheema, T.P. Martens, Q. Al-Awqati, The renal papilla is a niche for adult kidney stem cells, J. Clin. Invest. 114 (2004) 795-804. doi:10.1172/JCI20921.
[28] T.B. Kurth, F. Dell'Accio, V. Crouch, A. Augello, P.T. Sharpe, C. De Bari, Functional mesenchymal stem cell niches in adult mouse knee joint synovium in vivo, Arthritis Rheum. 63 (2011) 1289-300. doi:10.1002/art.30234.
[29] C.K.F. Chan, C.C. Chen, C.A. Luppen, J.B. Kim, A.T. DeBoer, K. Wei, J.A. Helms, C.J. Kuo, D.L. Kraft, I.L. Weissman, Endochondral ossification is required for haematopoietic stem-cell niche formation, Nature. 457 (2009) 490-4. doi:10.1038/nature07547.
[30] M.A. Scott, B. Levi, A. Askarinam, A. Nguyen, T. Rackohn, K. Ting, C. Soo, A.W. James, Brief Review of Models of Ectopic Bone Formation, Stem Cells Dev. 21 (2011) 655-67. doi:10.1089/scd.2011.0517.
[31] A. Trounson, C. McDonald, Stem Cell Therapies in Clinical Trials: Progress and Challenges, Cell Stem Cell. 17 (2015) 11-22. doi:10.1016/j.stem.2015.06.007.
[32] D. Fleifel, M.A. Rahmoon, A. AlOkda, M. Nasr, M. Elserafy, S.F. El-Khamisy, Recent advances in stem cells therapy: A focus on cancer, Parkinson's and Alzheimer's, J. Genet. Eng. Biotechnol. 16 (2018) 427-432. doi:10.1016/j.jgeb.2018.09.002.
[33] C. Loebel, J.A. Burdick, Engineering Stem and Stromal Cell Therapies for Musculoskeletal Tissue Repair, Cell Stem Cell. 22 (2018) 325-339. doi:10.1016/j.stem.2018.01.014.
[34] B. Gao, R. Deng, Y. Chai, H. Chen, B. Hu, X. Wang, S. Zhu, Y. Cao, S. Ni, M. Wan, L. Yang, Z. Luo, X. Cao, Macrophage-lineage TRAP+ cells recruit periosteum-derived cells for periosteal osteogenesis and regeneration, J. Clin. Invest. 129 (2019) 2578-2594. doi:10.1172/JCI98857.
[35] S. Debnath, A.R. Yallowitz, J. McCormick, S. Lalani, T. Zhang, R. Xu, N. Li, Y. Liu, Y.S. Yang, M. Eiseman, J.H. Shim, M. Hameed, J.H. Healey, M.P. Bostrom, D.A. Landau, M.B. Greenblatt, Discovery of a periosteal stem cell mediating intramembranous bone formation, Nature. 562 (2018) 133-139. doi:10.1038/s41586-018-0554-8.
[36] M.D. Brodt, C.B. Ellis, M.J. Silva, Growing C57B1/6 mice increase whole bone mechanical properties by increasing geometric and material properties, J. Bone Miner.

Res. 14 (1999) 2159-66. doi:10.1359/jbmr.1999.14.12.2159.
[37] J.M. Somerville, R.M. Aspden, K.E. Armour, K.J. Armour, D.M. Reid, Growth of C57Bl/6 Mice and the Material and Mechanical Properties of Cortical Bone from the Tibia, Calcif. Tissue Int. 74 (2004) 469-75. doi:10.1007/s00223-003-0101-x.

Figure 1

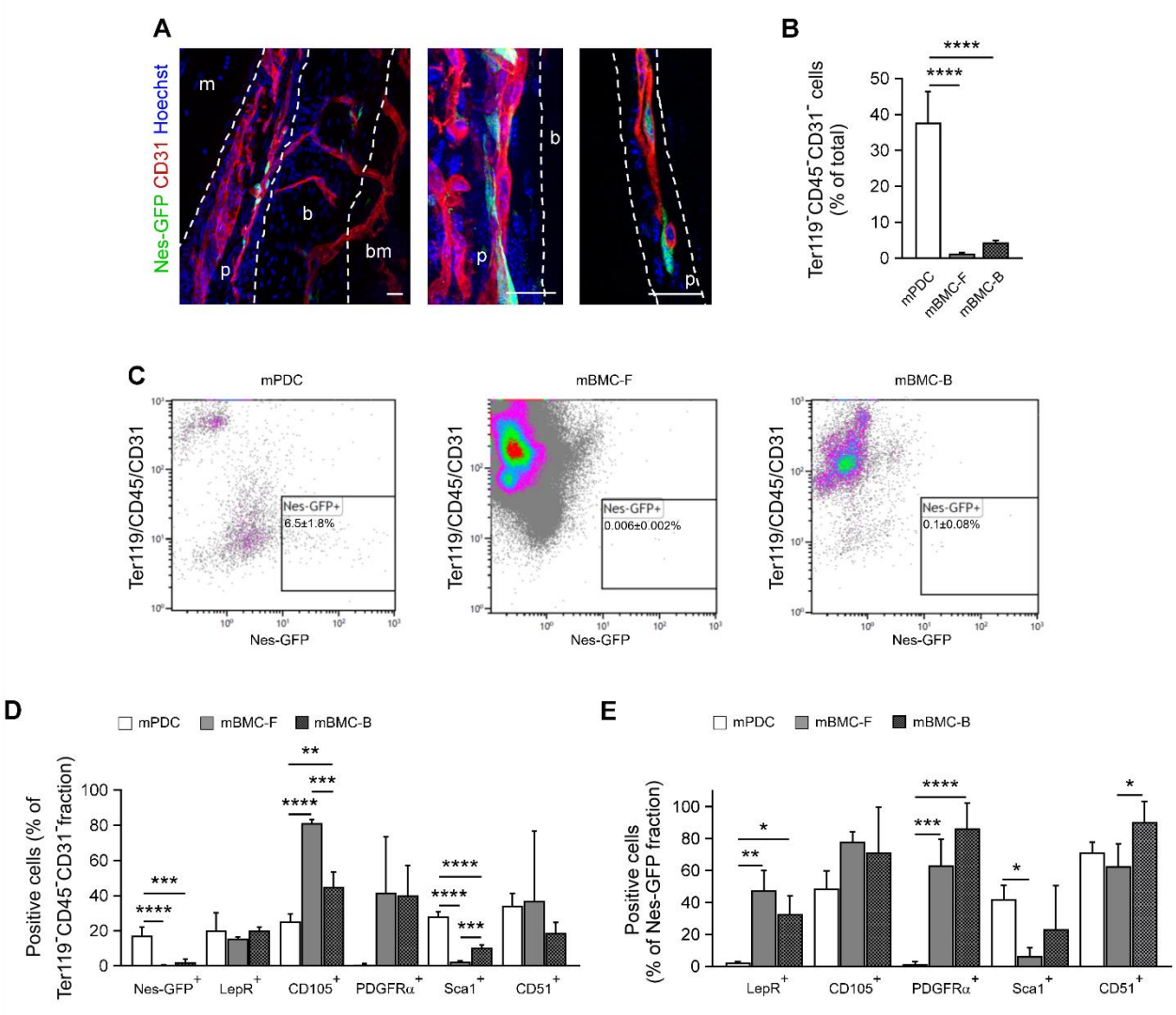

Figure1: Mouse periosteal and bone marrow-derived Nes-GFP$^+$ cells differ in stem cell and progenitor marker expression. (A) CD31-immunostaining of blood vessels in periosteum of Nes-GFP mice. Nuclei are stained with Hoechst (scale bar: 20µm; b, bone; bm, bone marrow; m, muscle; p, periosteum). (B) Flow cytometry analysis of periosteal cells (mPDC), flushed (mBMC-F) and digested (mBMC-B) bone marrow cells, with quantification of Ter119$^-$CD45$^-$ CD31$^-$ cells as stromal fraction. (C) Flow cytometry analysis of Nes-GFP$^+$Ter119$^-$CD45$^-$CD31$^-$ cells as percentage of total mPDC, mBMC-F and mBMC-B. (D-E) Flow cytometry analysis of

indicated markers with quantification of positive cells in the stromal fraction (C) or in Nes-GFP$^+$ fraction (D). Data are mean ± SD. n=4. *, p<0.05; **,p<0.01; ***, p<0.001; ****, p<0.0001 (one-way ANOVA).

Figure 2

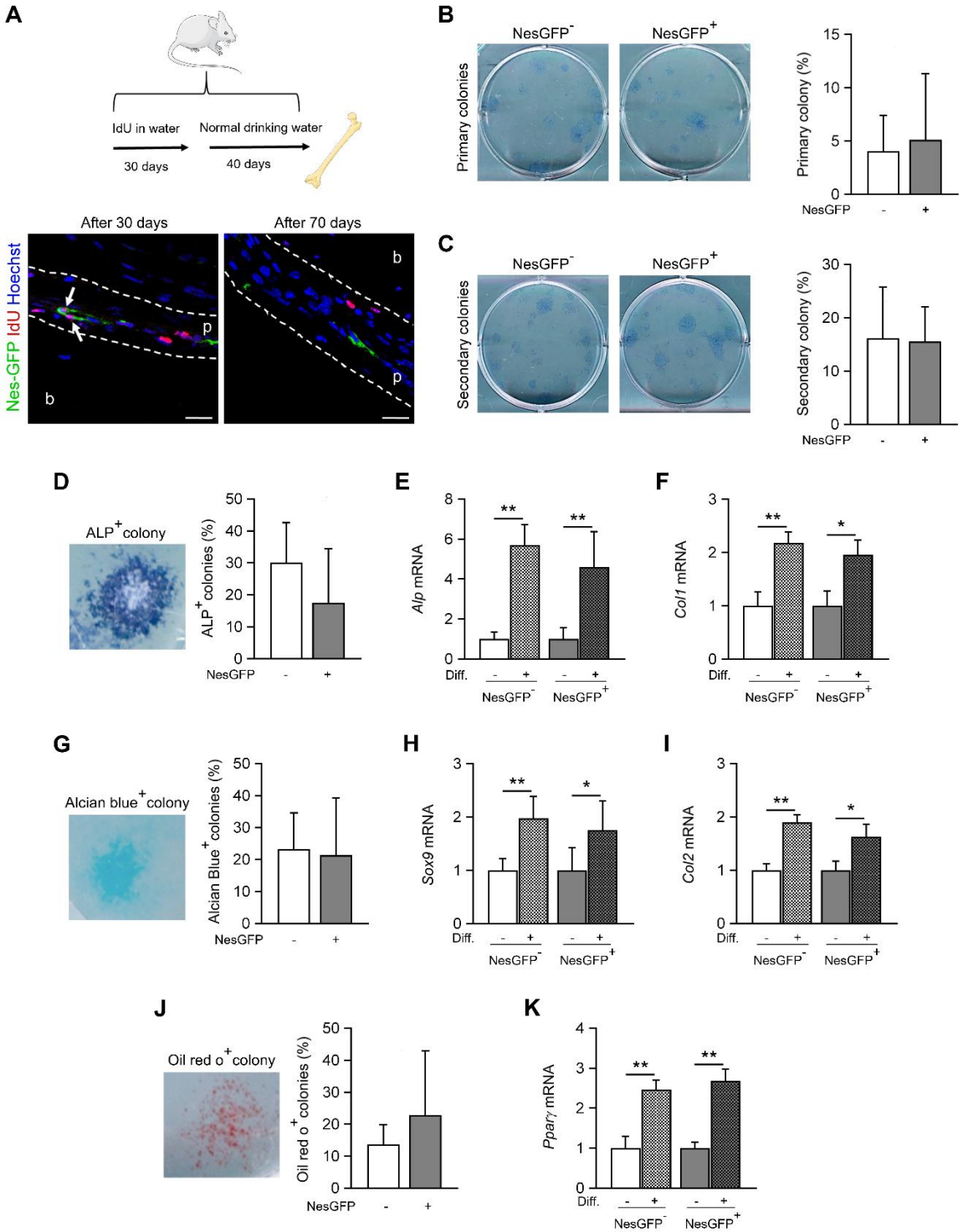
A
IdU in water
30 days
Normal drinking water
40 days
After 30 days
After 70 days
Nes-GFP IdU Hoechst
b
p
B
NesGFP-
NesGFP+
Primary colonies
Primary colony (%)
NesGFP
C
Secondary colonies
Secondary colony (%)
D
ALP+colony
ALP+colonies (%)
E
Alp mRNA
Diff.
F
Col1 mRNA
G
Alcian blue+colony
Alcian Blue+colonies (%)
H
Sox9 mRNA
I
Col2 mRNA
J
Oil red o+colony
Oil red o+colonies (%)
K
Pparγ mRNA

Figure 2: Nes-GFP is expressed by skeletal progenitors in the periosteum. (A) Experimental set-up (top panel) and anti-IdU staining on Nes-GFP femur (bottom panel), after IdU administration for 30 days and after a chase period of 40 days (70 days). Nuclei are stained by Hoechst (arrows point to Nes-GFP$^+$/IdU$^+$ cells). (B, C) Methylene Blue staining and quantification of primary (B) and secondary (C) colony formation by sorted Ter119$^-$CD45$^-$CD31$^-$ NesGFP$^-$ and Ter119$^-$CD45$^-$CD31$^-$NesGFP$^+$ periosteal cells (B, n=8 ; C, n=6). (D) Osteogenic differentiation of sorted Nes-GFP$^-$ and Nes-GFP$^+$ periosteal cells shown by staining for alkaline phosphatase activity (ALP) and quantification of ALP$^+$ colonies (n=8). (E, F) *Alp* (E) and *Collagen1* (*Col1*) (F) gene expression in differentiated vs undifferentiated mPDC (n=3). (G) Chondrogenic differentiation of sorted Nes-GFP$^-$ and Nes-GFP$^+$ periosteal cells, shown by Alcian blue staining of proteoglycans and quantification of positive colonies (n=8). (H, I) *Sox9* (H) and *Collagen 2* (*Col2*) (I) gene expression in differentiated vs undifferentiated mPDC (n=3). (J) Adipogenic differentiation of sorted Nes-GFP$^-$ and Nes-GFP$^+$ periosteal cells, shown by Oil Red O staining and quantification of positive colonies (n=8). *Ppar*γ gene expression in differentiated vs undifferentiated mPDC (K) (n=3). Data are mean ± SD. *, p<0.05; **,p<0.01 ((B, C, D, G, J) paired t-test and (E, F, H, I, K) two ways ANOVA).

Figure 3

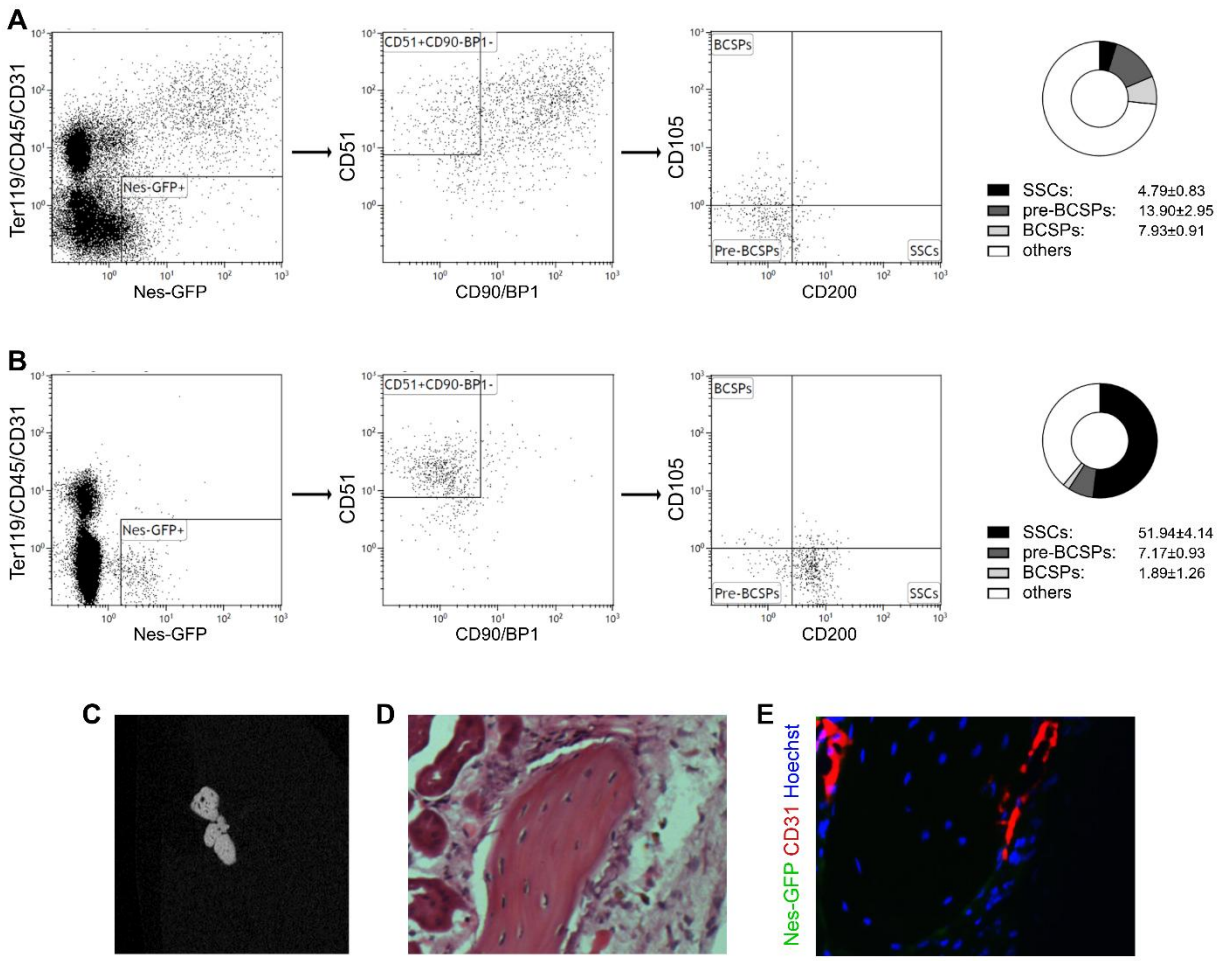

Figure 3: Periosteal Nes-GFP$^+$ cells are low in immunophenotypic SSCs and behave as osteoprogenitors *in vivo*. (A, B) Flow cytometry analysis of the proportion of Skeletal Stem Cells (SSCs; Ter119$^-$CD45$^-$CD31$^-$CD51$^+$CD90$^-$BP1$^-$CD105$^-$CD200$^+$), pre-Bone, Cartilage and Stromal Progenitors (pre-BCSPs; Ter119$^-$CD45$^-$CD31$^-$CD51$^+$CD90$^-$BP1$^-$CD105$^-$CD200$^-$) and Bone, Cartilage and Stromal Progenitors (BCSPs; Ter119$^-$CD45$^-$CD31$^-$CD51$^+$CD90$^-$BP1$^-$CD105$^+$CD200$^-$) in the Nes-GFP$^+$ fraction of periosteal cells (A) and flushed bone marrow cells after lineage and CD45 depletion (B). (C-E) Analysis of periosteal Nes-GFP$^+$ cells implanted beneath the kidney capsule. (C) µCT based visualization of mineralized tissue under the kidney

capsule 8 weeks after implantation. (D) Histological analysis (H&E staining) of bone formed under the kidney capsule. (E) Nes-GFP^{+} cells are not present in the implants 8 weeks post implantation. Scale bars are 20 μm. Data are mean ± SD. n=4.

Figure 4

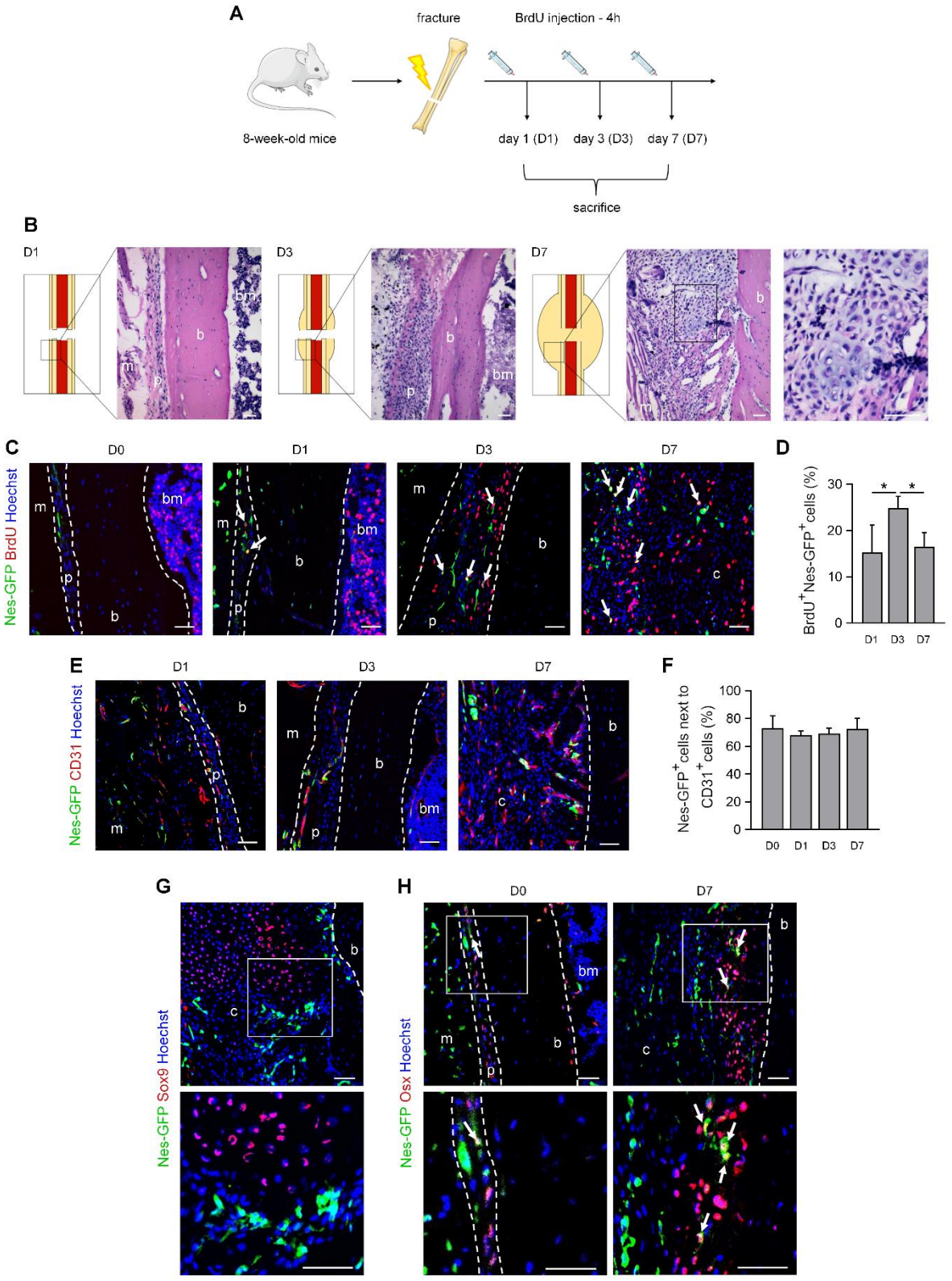

Figure 4: Nes-GFP$^+$ cells proliferate in response to fracture. (A) Scheme of experimental set-up. (B) H&E staining of the fractured tibia showing inflammatory response at day 1 (D1),

thickening of periosteum at D3 and initiation of callus formation at D7 (magnification of boxed area shows cartilage tissue). (C) Proliferating cells, shown by BrdU immunostaining, in the tibia of Nes-GFP mice before (D0) and after fracture (arrows point to proliferating Nes-GFP$^+$ cells). (D) Quantification of proliferating (BrdU$^+$) cells in the Nes-GFP$^+$ population (n=4). (E) CD31 immunostaining (blood vessels) on fractured tibia. (F) Quantification of Nes-GFP$^+$ cells in direct contact with CD31$^+$ cells (n = 4). (G) Sox9 immunostaining, showing chondrocytes in the callus, 7 days after fracture, which do not express Nes-GFP. (H) Osterix (Osx) immunostaining, showing osteoprogenitors in unfractured bone (D0) and 7 days after fracture. The boxed areas are enlarged in the lower panels (arrows point to Osx$^+$ Nes-GFP$^+$ cells). Nuclei are stained by Hoechst. b, bone; bm, bone marrow; c, callus; p, periosteum. Scale bars are 50 μm. Data are mean ± SD. *, $p<0.05$ (one-way ANOVA).